Archival Report

Biological Psychiatry: CNNI

Large-Scale Brain Network Dynamics Provide a Measure of Psychosis and Anxiety in 22q11.2 Deletion Syndrome

Daniela Zöller, Corrado Sandini, Fikret Işik Karahanoğlu, Maria Carmela Padula, Marie Schaer, Stephan Eliez, and Dimitri Van De Ville

ABSTRACT

BACKGROUND: Prodromal positive psychotic symptoms and anxiety are two strong risk factors for schizophrenia in 22q11.2 deletion syndrome (22q11DS). The analysis of large-scale brain network dynamics during rest is promising to investigate aberrant brain function and identify potentially more reliable biomarkers.

METHODS: We retrieved and examined dynamic properties of large-scale functional brain networks using innovation-driven coactivation patterns. The study included resting-state functional magnetic resonance scans from 78 patients with 22q11DS and 85 healthy control subjects. After group comparison of temporal brain network activation properties, functional signatures of prodromal psychotic symptoms and anxiety were extracted using multivariate partial least squares correlation.

RESULTS: Patients with 22q11DS had shorter activation in cognitive brain networks, longer activation in emotion processing networks, and generally increased segregation between brain networks. The functional signature of prodromal psychotic symptoms confirmed an implication of cingulo-prefrontal salience network activation duration and coupling. Further, the functional signature of anxiety uncovered an implication of amygdala activation and coupling, indicating differential roles of dorsal and ventral subdivisions of the anterior cingulate and medial prefrontal cortices. Coupling of amygdala with the dorsal anterior cingulate and medial prefrontal cortices was promoting anxiety, whereas coupling with the ventral anterior cingulate and medial prefrontal cortices had a protective function.

CONCLUSIONS: Using innovation-driven coactivation patterns for dynamic large-scale brain network analysis, we uncovered patterns of brain network activation duration and coupling that are relevant in clinical risk factors for psychosis in 22q11DS. Our results confirm that the dynamic nature of brain network activation contains essential function to develop clinically relevant imaging markers of psychosis vulnerability.

Keywords: 22q11.2 Deletion syndrome, Amygdala-prefrontal connectivity, Anxiety, Positive psychotic symptoms, Resting-state fMRI dynamics, Salience network

https://doi.org/10.1016/j.bpsc.2019.04.004

Schizophrenia is a strongly debilitating mental disorder both for affected individuals and in terms of societal cost (1,2). Converging evidence suggests that schizophrenia is a progressive neurodevelopmental disorder, given that, in most cases, subclinical psychiatric and cognitive symptoms of the disorder are present several years prior to the onset of a full-blown psychotic episode (1,3–7). The neurodevelopmental model critically implies that earlier interventions might prove more effective in preventing the progression toward psychosis (5,8). Hence, extensive research has been devoted to characterizing the prodromal disease stage, also known as psychosis high-risk state (3). In particular, the presence of attenuated positive psychotic symptoms, operationalized in the ultra-high-risk criteria (9), confers a strongly increased 30% to 40% risk of developing psychosis (10). While current clinical management is based purely on clinical observation (11,12), the identification of biomarkers of early psychosis could improve our understanding of the pathophysiology in its earliest disease stage (13). In this sense, the addition of imaging markers to the existing clinical diagnostic tools could allow the establishment of more precise biomarker-informed stages in the evolution of psychosis, which would give way to more targeted therapeutic strategies and improved clinical outcomes (1,8,13).

Chromosome 22q11.2 deletion syndrome (22q11DS) is a neurodevelopmental disorder that comes with a highly elevated risk for schizophrenia, with 30% to 40% prevalence by adulthood (14). Most patients with 22q11DS were diagnosed during childhood, which allows characterizing the earliest stages of schizophrenia's disease course (1,15).

SEE COMMENTARY ON PAGE 852

ISSN: 2451-9022

Similar to the general population, the presence of attenuated psychotic symptoms strongly increases the risk of psychosis in 22q11DS, pointing to a common clinical trajectory with nonsyndromic schizophrenia (16). Moreover, anxiety has emerged as another strong risk factor for psychosis in 22q11DS (17,18). These clinical findings point to the particular importance of understanding the pathophysiology and characterizing biomarkers of attenuated psychotic symptoms and anxiety in 22q11DS.

Among the tools to characterize biomarkers, resting-state functional magnetic resonance imaging (rs-fMRI) has emerged as promising (19). fMRI provides the unique opportunity to noninvasively observe brain function, and the resting condition is especially well suited in clinical populations because it requires minimal compliance from participants. Most studies on rs-fMRI in psychosis to date have used static functional connectivity (FC); i.e., the correlation between the activation in different brain regions over the whole scanning time (20). However, a limitation of such static approaches is that they ignore the inherently dynamic nature of brain activity, with potentially valuable information contained in dynamic changes of activation and connectivity (21–25). In this perspective, dynamic approaches have the potential to identify more precise and more reliable biomarkers, and these approaches are particularly promising in schizophrenia, given the multiplicity of affected behavioral domains and brain circuits (20,26–29). Studies on dynamic brain function in schizophrenia point toward disrupted dynamic interaction between several brain states, in particular, of subcortico-cortical connectivity (30) and connections of the default mode network (DMN) (31–34). The few studies to date investigating dynamic FC (dFC) in individuals at clinical high risk found reduced dFC of the salience network (SN) and DMN (35) and stronger alterations in early schizophrenia patients than subjects at ultra high risk (36), underlining the potential of dynamic brain function to improve our understanding of the pathophysiology in subjects at risk for schizophrenia.

Despite these promises of dynamic fMRI analysis, functional neuroimaging research in 22q11DS has so far mostly focused on static functional features (37–41), often targeting only specific networks such as the DMN (42,43). The studies that explicitly investigated psychotic symptoms in 22q11DS showed correlations of DMN dysconnectivity with prodromal psychotic symptoms (37), as well as successful discrimination between patients with high-risk– versus low-risk– based whole-brain rs-fMRI (38) and hypoconnectivity of the DMN, SN, anterior cingulate cortex (ACC), and frontoparietal network (FPN) (40). Further, in the only two studies to date investigating a dynamic feature of brain function in 22q11DS—the variability of blood oxygen level–dependent (BOLD) signals—we found widespread reductions in brain variability in 22q11DS (44) and reduced variability in the dorsal ACC (dACC) in patients with higher prodromal psychotic symptoms (45). In general, not only the aberrant function, but also the structure of the ACC have been suggested as neuroimaging markers for the development of psychosis in 22q11DS (46) and might reflect dysfunctional self-monitoring and salience processing, possible mechanisms for the emergence of psychosis (47).

Among the multiple methods to investigate dynamic fMRI (23), many have already been applied in schizophrenia as outlined above (26,36). Sliding-window dFC tracks changes in FC by computing FC in a temporal window that is shifted over time (21,34), but it is limited by the necessity to choose the window size and can only detect relatively slow changes in FC (48). Alternatively, so-called first-order approaches rely on temporal clustering of fMRI frames to obtain "coactivation patterns" (CAPs) (49). Here, even fast changes can be traced as no minimum activation duration needs to be specified. However, only one brain state (or CAP) can be active at a time point. To overcome these limitations, the recently introduced innovation-driven CAPs (iCAPs) framework detects moments of significantly changing brain activity to extract large-scale brain networks and their dynamic properties (25,50,51). Here, brain networks are retrieved from dynamic activation changes, which allows robust retrieval of spatially and temporally overlapping brain networks.

In this study, we complement the existing literature on dFC in schizophrenia by using iCAPs combined with multivariate pattern analysis to identify potential biomarkers for psychosis vulnerability in 22q11DS. We detect functional fingerprints of anxiety and positive prodromal symptoms, two symptoms that have emerged as reliable predictors of psychosis in 22q11DS (16,18).

METHODS AND MATERIALS

Participants

The study included 221 subjects (111 patients with 22q11DS, 110 healthy control [HC] subjects; both groups comprising individuals 8–30 years of age). We excluded 33 patients and 25 HC subjects to ensure good-data quality (see Supplementary Methods). The final sample included 78 patients with 22q11DS (37 males) and 85 HC subjects (36 males) (see Table 1). HC subjects were recruited among patients' siblings and through the Geneva state school system and had no present or past history of neurological or psychiatric disorders.

Prodromal positive psychotic symptoms in patients with 22q11DS were assessed using the Structured Interview for Prodromal Symptoms (52). The Structured Interview for Prodromal Symptoms was not conducted in HC subjects. Anxiety was assessed both in HC subjects and patients with 22q11DS by combining the Child Behavior Checklist Anxious-Depressed scale (53), and the Adult Behavior Checklist Anxious scale in adults above 18 years of age (54).

Participants and their parents (for minors) gave their written informed consent, and the research protocols were approved by the Institutional Review Board of Geneva University School of Medicine.

Image Acquisition

All MRI brain scans were acquired at the Centre d'Imagerie BioMédicale in Geneva on a Siemens Trio (12-channel coil; 54 HC subjects, 42 patients) (Siemens Healthineers, Erlangen, Germany) and a Siemens Prisma (20-channel coil; 31 HC subjects, 36 patients) (Siemens Healthineers) 3T scanner. Structural images were obtained with a T1-weighted sequence of 0.86 $mm^3 \times 0.86$ $mm^3 \times 1.1$ mm^3 volumetric resolution (192 coronal slices, repetition time = 2500 ms, echo time = 3 ms, acquisition matrix = 224 × 256, field of view = 22 cm^2, flip

Table 1. Participant Demographics

	HC Group (n = 85)	22q11DS Group (n = 78)	p Value
Gender, Male/Female	36/49	37/41	.514 (χ^2)
Age, Years	16.73 ± 5.85 (8.1–30.0)	17.19 ± 5.37 (8.1–29.7)	.603
Right-handed, %[a]	80.00	77.94	.715 (χ^2)
IQ[b]	110.12 ± 13.78	70.01 ± 12.41	<.001
Subjects Meeting Criteria for Any Psychiatric Diagnosis	N/A	43 (55)	
Anxiety disorder	N/A	9	
Attention-deficit/ hyperactivity disorder	N/A	8	
Mood disorder	N/A	5	
Schizophrenia or schizoaffective disorder	N/A	4	
More than one psychiatric disorder	N/A	17	
Subjects Medicated			
Methylphenidate	0	9	
Antipsychotics	0	3	
Anticonvulsants	0	1	
Antidepressants	0	1	
More than one class of medication	0	3	

Values are n, mean ± SD (range), mean ± SD, or n (%).

22q11DS, 22q11.2 deletion syndrome; HC, healthy control; N/A, not applicable.

[a]Measured using the Edinburgh laterality quotient, right-handedness was defined by a score of more than 50.

[b]Measured using the Wechsler Intelligence Scale for Children–III (100) for children and the Wechsler Adult Intelligence Scale–III (101) for adults.

angle = 8°). rs-fMRI data were recorded with a T2*-weighted sequence of 8 minutes (voxel size = 1.84 mm^3 × 1.84 mm^3 × 3.2 mm^3, 38 axial slices, repetition time = 2400 ms, echo time = 30 ms, flip angle = 85°). Subjects were instructed to fixate on a cross on the screen, let their mind wander, and not fall asleep.

Preprocessing

Before applying the iCAPs pipeline, MRI scans were preprocessed using SPM12 (http://www.fil.ion.ucl.ac.uk/spm/) and functions of the Data Processing Assistant for Resting-State fMRI (55) and Individual Brain Atlases using Statistical Parametric Mapping (56) toolboxes. After realignment of functional scans, we applied spatial smoothing with an isotropic Gaussian kernel of 6-mm full width at half maximum and coregistered structural scans to the functional mean. Structural images were segmented with the SPM12 Segmentation algorithm (57), and a study-specific template was generated using Diffeomorphic Anatomical Registration using Exponential Lie algebra (58). Then, the first five functional scans were excluded, and average white matter and cerebrospinal fluid signals were regressed out from the BOLD time series. We applied motion scrubbing (59) for correction of motion artifacts, marking frames with a framewise displacement of more than 0.5 mm. As the filters implemented in the iCAPs framework require a constant sampling rate, marked frames were replaced by the spline interpolation of previous and following frames. Finally, motion frames were excluded before computation of temporal characteristics (described below).

Total Activation and iCAPs

We used openly available MATLAB code (https://c4science.ch/source/iCAPs/) MATLAB vR2017a (The MathWorks, Inc., Natick, MA) to apply iCAPs (25,50,51). We first employed Total Activation (60–62), which applies hemodynamically informed deconvolution to the fMRI time series through spatiotemporal regularization. Significant activation changepoints (i.e., transients), derived from deconvolved time series, were concatenated across all subjects and fed into temporal k-means clustering to obtain simultaneously transitioning brain patterns, the iCAPs. The optimum number of 17 clusters was determined by consensus clustering (63) (see Supplemental Figures S1 and S2). Finally, time courses were obtained for all iCAPs using spatiotemporal transient-informed regression (51). A detailed description of all steps can be found in the Supplementary Methods.

Extraction of Temporal Properties

For computation of temporal properties, iCAPs time courses were Z-scored within each subject and thresholded at a Z score $>|1|$ to determine "active" time points (50). For each iCAP, we then computed the total duration of overall activation as percentage of the total nonmotion scanning time.

Further, coupling and anticoupling duration of two iCAPs were calculated as time points of same-signed or oppositely signed coactivation measured as percentage of the total nonmotion scanning time or as Jaccard score; i.e., percent joint activation time of the two respective iCAPs.

Statistical Analysis

Group Comparisons of iCAPs Activation Measures. Duration and coupling measures between groups were compared using two-sample t tests. The p values were corrected for multiple comparisons with the false discovery rate.

Partial Least Squares Correlation. To evaluate multivariate patterns of correlation between behavioral variables and iCAPs activation measures, we used behavior partial least squares correlation (PLSC) (64). Briefly, we first computed a correlation matrix between behavioral variables and brain variables. Group-specific correlation matrices of HC subjects and patients with 22q11DS were concatenated, and singular value decomposition of this matrix then led to several correlation components (CorrComps). Each CorrComp is composed of a set of behavior weights and iCAPs duration/coupling weights, which indicate how strongly each variable contributes to the multivariate brain-behavior correlation. Significance of CorrComps was determined by permutation testing (1000 permutations). Stability of brain and behavior weights was

obtained using bootstrapping (500 bootstrap samples). See the Supplementary Methods for a detailed outline of PLSC.

Here, we first conducted two PLSC analyses, with duration of altered iCAPs as brain variables and with psychotic symptoms (in the first PLSC analysis) and anxiety (in the second PLSC analysis) as behavioral variables. In four more PLSC analyses, we then investigated positive couplings and anticouplings of one selected iCAP for each behavioral measure. Owing to differences in design of each PLSC in terms of measure type and number of items, we did not correct for multiple comparisons.

Nuisance Variable Regression. Age, gender, and motion were included as nuisance regressors in group comparisons and PLSC analyses. Nuisance regressors were standardized within each group to avoid linear dependence with the effects of interest.

RESULTS

Extracted Spatial Maps Correspond to Known Resting-State Networks

We applied the iCAPs framework to rs-fMRI scans of both HC subjects and patients with 22q11DS. Identified iCAPs correspond to well-known resting-state networks (see Figure 1 and Supplemental Table S2). The obtained networks included sensory-related networks such as primary visual 1 and 2, secondary visual, auditory/sensorimotor, and sensorimotor networks. The DMN was decomposed into anterior, posterior, and precuneus/ventral DMN. There were two attention-related iCAPs, i.e., the FPN and visuospatial network. Two iCAPs included regions commonly considered as the SN: the anterior insula and dACC together with dorsolateral prefrontal cortex (dlPFC). The remaining iCAPs comprised a language network (LAN), inferior temporal and fusiform (iTEMP/FUS), amygdala and hippocampus (AMY/HIP), orbitofrontal cortex, and PFC.

Altered iCAPs' Activation and Coupling in 22q11DS

To probe into alterations of the identified networks' temporal properties in patients with 22q11DS, we first investigated aberrant activation duration followed by the analysis of altered network interactions; i.e., duration of positive coupling (coactivation with same sign) or anticoupling (coactivation with opposite sign) between all pairwise combinations of iCAPs.

Altered Duration of iCAPs' Activation. Figure 2 shows duration for all 17 iCAPs in percentage of total nonmotion scanning time. Median total activation time ranged from 34.36% for the LAN to 1.54% for the PFC. Patients with 22q11DS had significantly shorter activation of the dACC/dlPFC, primary visual 2 network, FPN, anterior DMN (aDMN), and posterior DMN and significantly longer activation of the sensorimotor network, iTEMP/FUS, AMY/HIP, and orbitofrontal cortex.

Alterations in Coupling Between Networks. Figure 3 shows significant group differences in iCAPs' coupling. For several networks, the duration of coupling was longer in patients with 22q11DS than in control subjects. This was true for six positive couplings and 13 anticouplings. Fewer networks had shorter duration of coupling in patients with 22q11DS (one positive coupling, five anticouplings). Globally, alterations were more numerous for anticouplings (25 in total) than for positive couplings (six in total).

Functional Signature of Positive Psychotic Symptoms

To look into the behavioral relevance of these aberrant activation and coupling, we conducted behavior PLSC including positive symptoms.

Altered iCAPs' Duration Associated With Psychotic Symptoms. A first PLSC analysis including positive Structured Interview for Prodromal Symptoms items in 22q11DS and iCAPs' activation duration of the nine altered iCAPs (see Figure 2) resulted in one significant CorrComp (p = .05) (see Figure 4A). Duration of the dACC/dlPFC, FPN, and iTEMP/FUS was positively correlated with all five positive psychotic symptoms.

Altered Couplings of dACC/dlPFC Associated With Psychotic Symptoms. Next, we investigated the relevance of couplings for psychotic symptoms. For this, we selected the dACC/dlPFC network based on its appearance in the previous analysis (see Figure 4A), as well as literature associating ACC alterations with psychosis in 22q11DS (46). We included coupling time of the dACC/dlPFC with iCAPs that had altered couplings (anterior insula, auditory/sensorimotor network, iTEMP/FUS, and AMY/HIP) (see Figure 3) and with iCAPs whose duration was significantly correlated with psychotic symptoms (FPN and iTEMP/FUS) (see Figure 4A).

A first PLSC analysis for anticoupling time between the dACC/dlPFC and these networks resulted in one significant CorrComp (p = .02) (see Figure 4B) showing an association between higher positive symptoms and longer anticoupling of the dACC/dlPFC with FPN and iTEMP/FUS.

A second PLSC analysis for positive coupling time between dACC/dlPFC and these networks did not give any significant CorrComp (p = .58).

Functional Signature of Anxiety

Finally, we conducted similar analyses to investigate dynamic brain network alterations associated with anxiety, another behavioral risk factor for psychosis in 22q11DS.

Altered iCAPs' Duration Associated With Anxiety. We performed PLSC analysis between Child Behavior Checklist/Adult Behavior Checklist anxiety scores in 22q11DS and HC subjects and iCAPs' duration, again including the nine iCAPs with altered duration (see Figure 2). There was one significant CorrComp (p = .03) (see Figure 5A). In both HC subjects and patients with 22q11DS, longer activation of iTEMP/FUS and AMY/HIP and shorter activation of aDMN were associated with higher anxiety.

Altered Couplings of AMY/HIP Associated With Anxiety. To further investigate coupling effects related to anxiety, we selected the AMY/HIP network because its duration was related to anxiety in the previous analysis (see

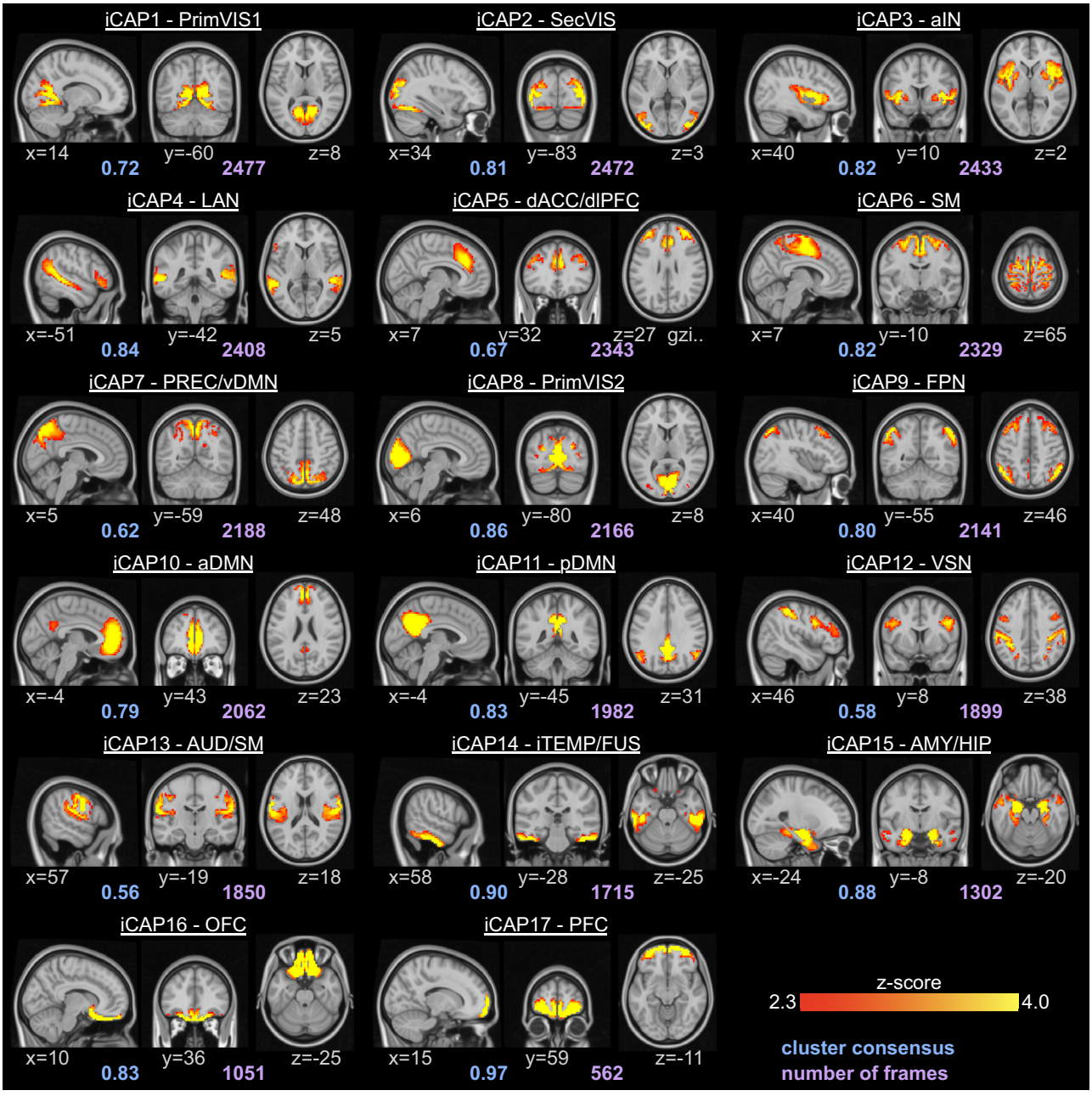

Figure 1. Spatial patterns of the 17 innovation-driven coactivation patterns (iCAPs) retrieved from all subjects, including both healthy control (HC) subjects and patients with 22q11.2 deletion syndrome (22q11DS). Locations denote displayed slices in Montreal Neurological Institute coordinates. Blue values denote the average consensus of each cluster, and purple values indicate the total number of innovation frames that were assigned to this cluster. aDMN, anterior default mode network; aIN, anterior insula; AMY/HIP, amygdala/hippocampus; AUD/SM, auditory/sensorimotor; dACC/dlPFC, dorsal anterior cingulate cortex/dorsolateral prefrontal cortex; FPN, frontoparietal network; iTEMP/FUS, inferior temporal/fusiform; LAN, language network; OFC, orbitofrontal cortex; pDMN, posterior default mode network; PFC, prefrontal cortex; PREC/vDMN, precuneus/ventral default mode network; PrimVIS1, primary visual 1; PrimVIS2, primary visual 2; SecVIS, secondary visual; SM, sensorimotor; VSN, visuospatial network.

Figure 5A) and because of the well-established involvement of these brain regions in anxiety (65). We included coupling time of AMY/HIP with iCAPs that had altered couplings (LAN, dACC/dlPFC, precuneus/ventral DMN, and FPN) (see Figure 3) and with iCAPs whose duration was significantly associated with anxiety (aDMN and iTEMP/FUS) (see Figure 5A).

A first PLSC analysis for anticouplings between AMY/HIP and these networks gave no significant CorrComp (p = .07).

A second PLSC analysis including positive couplings between AMY/HIP, and these networks gave one significant CorrComp (p = .006) (see Figure 5B). Behavior weights were only robust for patients with 22q11DS, indicating that the

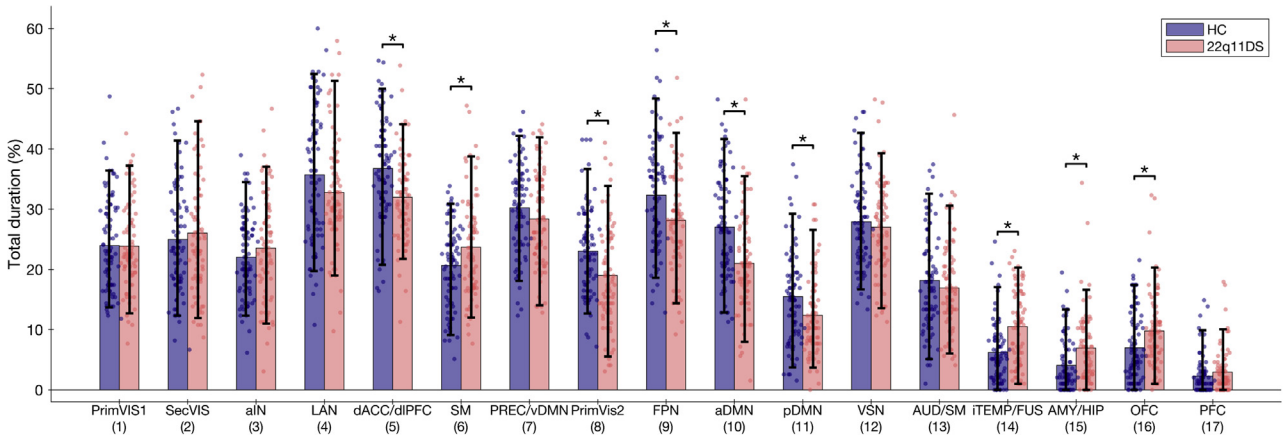

Figure 2. Statistics of total temporal duration for each innovation-driven coactivation pattern. The *p* values are false discovery rate corrected for the 17 multiple comparisons, and age, gender, and motion were included as covariates. Significant group differences ($p < .05$) were marked with an asterisk. Error bars indicate bootstrapping 5th to 95th percentiles. Single-subject duration measures were included as scatterplots. Corresponding test statistics (*p* values, effect size) can be found in Supplemental Table S3. 22q11DS, 22q11.2 deletion syndrome; aDMN, anterior default mode network; aIN, anterior insula; AMY/HIP, amygdala/hippocampus; AUD/SM, auditory/sensorimotor; dACC/dlPFC, dorsal anterior cingulate cortex/dorsolateral prefrontal cortex; FPN, frontoparietal network; HC, healthy control; iTEMP/FUS, inferior temporal/fusiform; LAN, language network; OFC, orbitofrontal cortex; pDMN, posterior default mode network; PFC, prefrontal cortex; PREC/vDMN, precuneus/ventral default mode network; PrimVIS1, primary visual 1; PrimVIS2, primary visual 2; SecVIS, secondary visual; SM, sensorimotor; VSN, visuospatial network.

corresponding pattern of correlation weights was specific for patients. Longer positive coupling of AMY/HIP with LAN and dACC/dlPFC was positively associated with anxiety, whereas positive coupling with aDMN was negatively associated with anxiety.

DISCUSSION

In this study, we investigated dynamic features of network brain activity in patients with 22q11DS, with a particular focus on the identification of functional signatures of prodromal psychotic symptoms and anxiety, two behavioral risk factors for the transition to psychosis. To the best of our knowledge, this is the first study to investigate dynamics of large-scale functional brain networks in 22q11DS. We used iCAPs to go beyond static connectivity analysis and look into precise moments of brain network activation and interaction, which is particularly promising to provide more sensitive imaging markers in schizophrenia (26). We detected alterations of brain networks' duration and couplings in 22q11DS and associations between these patterns of alterations with positive psychotic symptoms and anxiety.

Alterations in 22q11DS: Implication of Cognitive and Emotional Brain Networks

Individuals with 22q11DS had a varied pattern of longer and shorter network activations, suggesting that they "overengage" in certain brain states while "underengaging" in others. In particular, we found shorter activation of the FPN, DMN, and cingulo-prefrontal SN. According to the triple-network hypothesis, the dynamic interaction among these three networks, characterized by a shift between the internally oriented DMN and externally oriented FPN mediated by the salience-attributing SN, is central for higher cognitive functions (66). Conversely, their dysfunction could account for several psychiatric symptoms. Here, we observe reduced activation of all three networks in 22q11DS, possibly suggesting a malfunction of these basic brain dynamics, which speculatively may underlie broad impairments in higher cognitive function described in both 22q11DS and psychosis (1,67). In turn, there was longer activation in networks comprising limbic regions including the AMY, medial temporal, and orbitofrontal cortices. While the dichotomy between the cognitive and emotional brain is arguably artificial, longer activation in regions highly involved in emotional processing such as the AMY and orbitofrontal cortex could reflect higher emotional load during scanning in patients with 22q11DS (68,69).

The pattern of activation was significantly, but oppositely, related to age in both groups (see Supplementary Results and Discussion), suggesting that the atypical activation pattern observed in 22q11DS emerges with age, in accordance with the neurodevelopmental model of schizophrenia (1,6).

Besides duration of activation, the iCAPs approach allowed us to probe the pattern of aberrant coupling between networks, which was characterized by predominantly longer anticouplings in 22q11DS, accounting for more than half (13 of 25) of the alterations. Longer anticoupling is suggestive of increased segregation between brain networks and is in agreement with evidence of increased segregation and decreased integration of structural and functional brain networks in both 22q11DS and nonsyndromic psychosis (20,70–74). Network segregation is a central feature of brain function that is important for cognition and attention (75), and its alterations in 22q11DS may be reflective of cognitive disabilities on a more global level than the above-mentioned alterations in triple-network activation that concentrates on three core networks.

Functional Signature of Psychosis Prodromal: Aberrant SN Duration and Coupling

The presence of prodromal psychotic symptoms was associated with longer activation of the iTEMP/FUS, dACC/dlPFC,

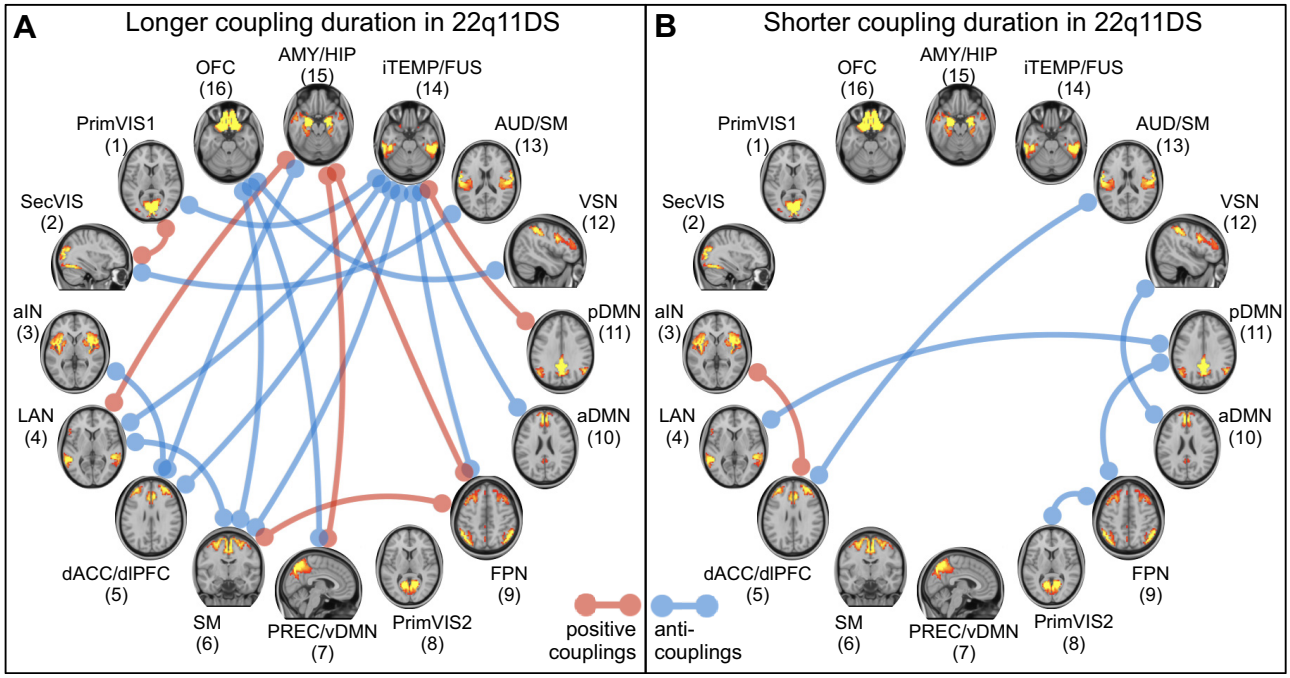

Figure 3. Significant duration differences of positive couplings (red) and anticouplings (blue) between patients with 22q11.2 deletion syndrome (22q11DS) and healthy control subjects. **(A)** Couplings with significantly longer duration in 22q11DS. **(B)** Couplings with significantly shorter duration in 22q11DS. Couplings were measured in terms of percentage of total scanning time or in percentage of the joint activation time of the two respective innovation-driven coactivation patterns (iCAPs) (Jaccard score). We here show only differences that were significant in both coupling measures. Underlying group comparison statistics can be found in Supplemental Figure S4 and Supplemental Table S4. aDMN, anterior default mode network; aIN, anterior insula; AMY/HIP, amygdala/hippocampus; AUD/SM, auditory/sensorimotor; dACC/dlPFC, dorsal anterior cingulate cortex/dorsolateral prefrontal cortex; FPN, frontoparietal network; iTEMP/FUS, inferior temporal/fusiform; LAN, language network; OFC, orbitofrontal cortex; pDMN, posterior default mode network; PREC/vDMN, precuneus/ventral default mode network; PrimVIS1, primary visual 1; PrimVIS2, primary visual 2; SecVIS, secondary visual; SM, sensorimotor; VSN, visuospatial network.

and FPN. Increased activation of the iTEMP/FUS has been previously reported in schizophrenia in terms of relative cerebral blood flow (76,77) and BOLD variability (78). Also in 22q11DS, we observed higher BOLD variability in the iTEMP/FUS regions in a partially overlapping sample (44), suggesting that increased BOLD variability might reflect longer network activation. Further, prodromal psychotic symptoms were associated with longer activation of dACC/dlPFC. The dACC is considered a key node of the SN involved in attributing subjective salience to internally and externally generated events (66,79). Aberrant salience attribution has been proposed as key mechanism in the emergence of positive psychotic symptoms (47). Together with electroencephalogram studies in psychosis and 22q11DS that consistently reported longer representation of the electroencephalogram topography that corresponds to SN (80–83), our findings support this hypothesis.

However, while duration of both dACC/dlPFC and FPN was positively correlated with psychotic symptoms, it was reduced overall in 22q11DS compared with HC subjects. Converging evidence from both structural and functional MRI points toward altered connectivity of the ACC in individuals with 22q11DS and psychotic symptoms (38,45,71,84), reviewed in Padula *et al.* (46). Hence, we suspected that the quality of the activations, i.e., the coupling with other networks, might be relevant for higher psychotic symptoms. Indeed, the analysis of dACC/dlPFC couplings revealed a significant relationship between higher psychotic symptoms and anticoupling with the FPN and iTEMP/FUS. Taken together, these results suggest that while activations of the dACC/dlPFC and FPN occur less frequently in 22q11DS in general, they are more frequently anticoupled with one another and with the iTEMP/FUS in patients with higher psychotic symptoms. The triple-network model proposes that activation of the SN is instrumental in reorienting attention by mediating the shifts between the DMN and FPN (66). Our findings of longer anticoupling between SN and FPN suggest that this functional role of the cingulo-prefrontal SN is disrupted in individuals with higher psychotic symptoms.

Altogether, the richness of our iCAPs approach permitted to characterize a pattern reflecting SN activations that contribute to the pathophysiology of psychotic symptoms, in terms of both duration and quality. Our findings support the key role of network dynamics in the ACC in higher psychosis vulnerability (46) and point toward disrupted triple-network function centered on the SN, which might reflect aberrant salience processing in patients with psychotic symptoms (47,66).

Functional Signature of Anxiety: Aberrant AMY/HIP Duration and Coupling

For both HC subjects and patients with 22q11DS, anxiety was associated with a pattern of longer activation of the AMY/HIP and iTEMP/FUS and shorter activation of the aDMN. Evidence

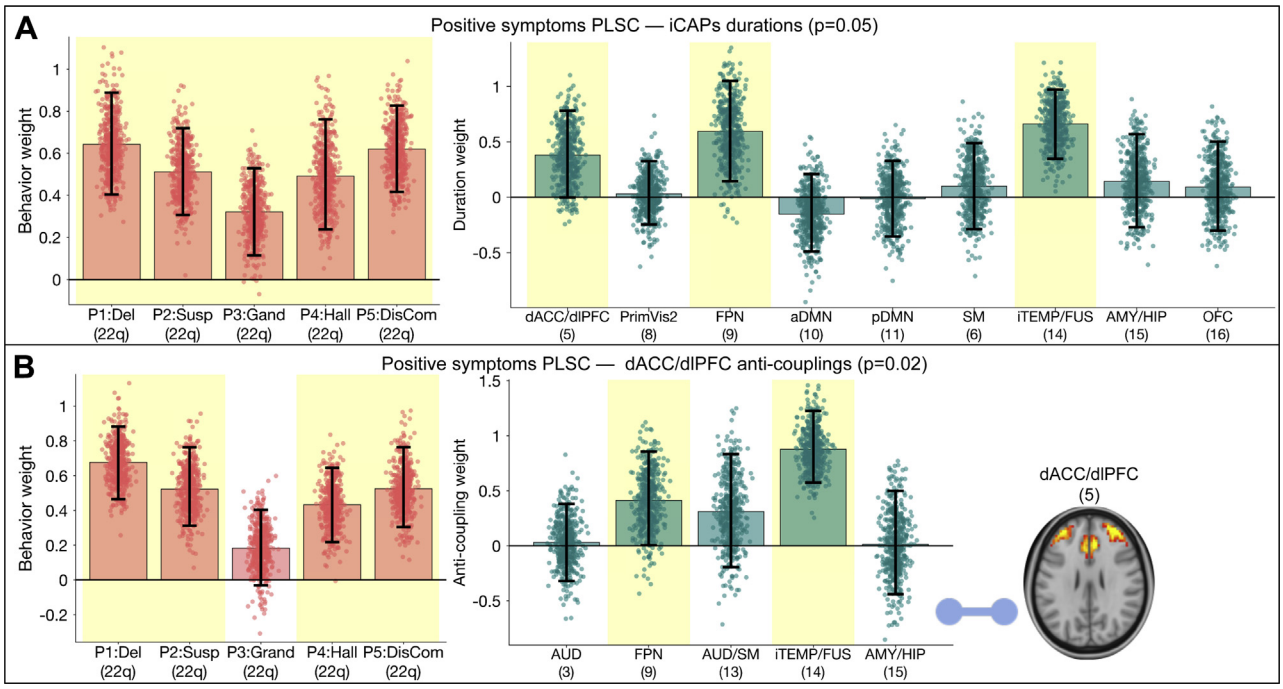

Figure 4. Partial least squares correlation (PLSC) results for positive psychotic symptoms (five Structured Interview for Prodromal Symptoms items: P1:Del, delusions; P2:Susp, suspiciousness; P3:Grand, grandiosity; P4:Hall, hallucinations; and P5:DisCom, disorganized communication) in patients with 22q11.2 deletion syndrome (22q). **(A)** Behavior weights and brain weights for PLSC including duration of nine innovation-driven coactivation patterns (iCAPs) with altered duration in 22q. There is a positive correlation of positive psychotic symptoms with duration of the dorsal anterior cingulate cortex/dorsolateral prefrontal cortex (dACC/dlPFC), frontoparietal network (FPN), and inferior temporal/fusiform (iTEMP/FUS). **(B)** Behavior weights and brain weights for PLSC including anticouplings of the dACC/dlPFC that were altered in 22q. Longer anticoupling of the dACC/dlPFC with the FPN and iTEMP/FUS is associated with higher positive symptoms. Error bars indicate bootstrapping fifth to 95th percentiles and robust results were indicated by yellow background. Exact values of bootstrap mean and fifth to 95 percentiles are reported in Supplemental Table S5. PLSC results for positive couplings were not significant (p = .6) and are thus not reported here. aDMN, anterior default mode network; AMY/HIP, amygdala/hippocampus; AUD, auditory; OFC, orbitofrontal cortex; pDMN, posterior default mode network; PrimVIS2, primary visual 2; SM, sensorimotor.

in animal models and humans has revealed a central role of the amygdala in fear exposure, anticipation, and reaction (65,68,85–88). Further, increased metabolic activity in the AMY, HIP, and iTEMP cortex was found in rhesus monkeys with anxious temperament (89,90), and cerebral blood flow in the AMY and FUS cortex has been associated with trait anxiety in humans (91). The iCAPs approach allowed us to quantify moments of network activation and confirmed that hyperactivity of the AMY/HIP and iTEMP/FUS at rest could indeed represent trait markers of anxiety in both HC subjects and 22q11DS. Hyperactivity of the AMY/HIP and iTEMP/FUS observed in 22q11DS could therefore account for increased prevalence of anxiety disorders in this population.

Importantly, the AMY does not operate in isolation, but is part of a complex circuit involved in regulating emotional responses (92). Indeed, in accord with the role in salience processing mentioned above, the dACC and mPFC promote amygdala activity and are critical in the appraisal and expression of fear behavior (92). Oppositely, the subgenual ACC and ventral mPFC largely dampen amygdala activity and are essential for fear extinction (92). This functional subdivision of the frontal lobe is further supported by extensive literature on fear circuitry in rodents, in which the dorsal prelimbic and ventral infralimbic cortices are found to have opposing roles on AMY activation and fear expression, and fear extinction, respectively (85,92–98). Given these findings, we speculated that the modulation of AMY/HIP activity, particularly by the dACC/dlPFC and aDMN network, might play a crucial role in the pathophysiology of anxiety. Indeed, we showed a significant positive association between anxiety and coupling duration between the AMY/HIP and dACC/dlPFC and the LAN. Coupling duration between the AMY/HIP and aDMN had an opposite, protective role on anxiety in accordance with the modulating role of mPFC-AMY projections on fear expression. Of note, the effects of AMY coupling on anxiety appeared specific to individuals with 22q11DS, which could suggest that effects of amygdala modulation are nonlinear and relate only to more severe anxiety observed in 22q11DS.

In conclusion, we observed a dynamic functional pattern characterized both by longer AMY/HIP activations and atypical prefrontal AMY/HIP modulation, which might constitute a trait maker of anxiety and contribute vulnerability to psychosis in 22q11DS.

Methodological Aspects

iCAPs Framework. The present study is one of the first to apply the iCAPs framework in a clinical population, and owing to the flexibility of the framework, we were able to discover distinct patterns of functional activation and interaction

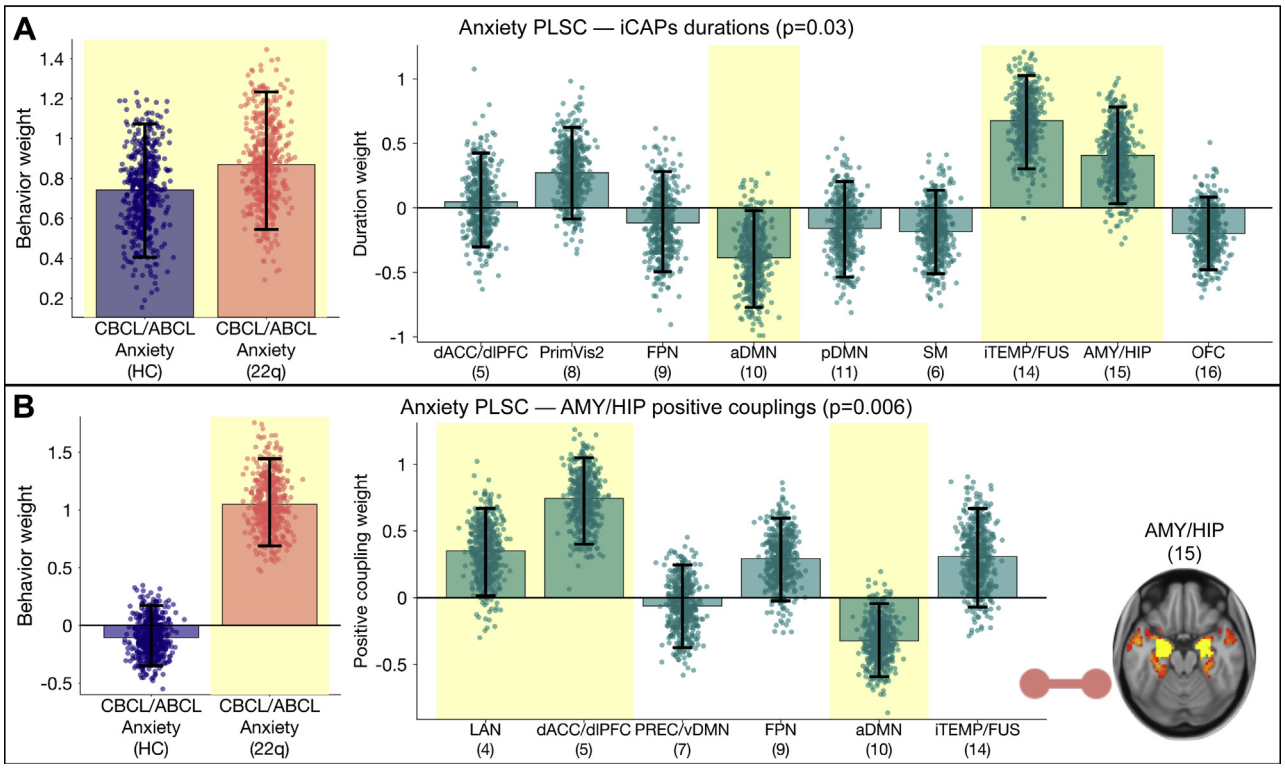

Figure 5. Partial least squares correlation (PLSC) results for anxiety scores. **(A)** Behavior weights and brain weights for PLSC including duration of nine altered innovation-driven coactivation patterns (iCAPs). There is a positive correlation of anxiety with duration of the inferior temporal/fusiform (iTEMP/FUS) and amygdala/hippocampus (AMY/HIP) and a negative correlation with duration of the anterior default mode network (aDMN). **(B)** Behavior weights and brain weights for PLSC including positive couplings of the AMY/HIP. Longer positive coupling of AMY/HIP with the language network (LAN) and dorsal anterior cingulate cortex/dorsolateral prefrontal cortex (dACC/dlPFC), and shorter positive coupling with the aDMN are associated with higher anxiety only in patients with 22q11.2 deletion syndrome (22q). Error bars indicate bootstrapping fifth to 95th percentiles, robust results were indicated by yellow background. Exact values of bootstrap mean and fifth to 95th percentiles are reported in Supplemental Table S6. PLSC results for anticouplings were not significant (p = .07) and are thus not reported here. ABCL, Adult Behavior Checklist; CBCL, Child Behavior Checklist; FPN, frontoparietal network; OFC, orbitofrontal cortex; pDMN, posterior default mode network; PREC/vDMN, precuneus/ventral default mode network; PrimVIS2, primary visual 2; SM, sensorimotor.

characteristic for prodromal psychotic symptoms and anxiety. The framework is unique in its ability to detect spatially and temporally overlapping networks (50,51), and the robustness and richness of the presented results underlines its potential. Of note, extracted spatial patterns were highly similar to previously observed iCAPs retrieved from HC subjects (50,51), which reassures the framework's performance in a clinical population. Furthermore, the subdivision of classical resting-state networks such as the DMN and SN into multiple subnetworks confirms previously observed findings (50) and suggests that different subnetworks have distinct dynamic properties, which are difficult to detect by static approaches.

While iCAPs themselves were retrieved from a purely dynamic measure (i.e., the innovations), the measure of coupling between networks is closely linked to static FC (see the Supplementary Results and Discussion). Activation duration, however, is a measure specific to each network, which cannot be explained in terms of static connectivity.

BOLD Signal Analysis and Motion. In any fMRI study, nonneural confounds are always a concern (99). We have minimized the effects by taking several measures for motion correction and through additional analysis of motion (discussed in more detail in the Supplementary Results and Discussion). However, as motion is strongly correlated with symptoms severity, it remains a limitation of our study.

Conclusions

In summary, we presented here functional signatures of anxiety and positive psychotic symptoms in 22q11DS in terms of brain network activation and coupling. Our results confirm the implication of SN activity and connectivity in the emergence of psychotic symptoms. We further uncovered differential roles of dACC and ventral ACC and mPFC coupling with the AMY that are relevant for anxiety. Together, these findings shed light into the pathophysiology of two clinical risk factors that might represent relevant imaging markers for psychosis vulnerability.

ACKNOWLEDGMENTS AND DISCLOSURES

This work was supported by the Swiss National Science Foundation Grant Nos. 32473B 121966 (to SE), 234730 144260 (to SE), 145250 (to SE), and 163859 (to MS); and National Center of Competence in Research "SYNAPSY - The Synaptic Bases of Mental Diseases," Swiss National Science Foundation, Grant Nos. 51AU40 125759 (to MCP, MS, and SE), 51NF40 158776 (to DZ, CS, MCP, MS, and SE), and 51NF40-185897 (to DZ, CS, MCP, MS, and SE).

We are grateful to the subjects who participated in our study and thank Sarah Menghetti, Léa Chambaz, Virginie Pouillard, and Dr. Maude Schneider for their involvement with the participants. We would also like to acknowledge Professor François Lazeyras and the Centre d'Imagerie BioMédicale group for their support during data collection.

All authors report no biomedical financial interests or potential conflicts of interest.

ARTICLE INFORMATION

From the Medical Image Processing Laboratory (DZ, DVDV), Institute of Bioengineering, École Polytechnique Fédérale de Lausanne, Lausanne; Department of Radiology and Medical Informatics (DZ, DVDV) and Developmental Imaging and Psychopathology Laboratory (DZ, CS, MCP, MS, SE), Department of Psychiatry, University of Geneva, Geneva; and the Friedrich Miescher Institute for Biomedical Research (MCP), Basel, Switzerland; and the Department of Radiology (FIK), Massachusetts General Hospital, Harvard Medical School, Boston; and Athinoula A. Martinos Center for Biomedical Imaging (FIK), Massachusetts General Hospital, Harvard Medical School, Charlestown, Massachusetts.

Address correspondence to Daniela Zöller, M.Sc., Institute of Bioengineering, EPFL, Department of Psychiatry, University of Geneva, Chemin des Mines 9, 1202 Geneva, Switzerland; E-mail: daniela.zoller@epfl.ch.

Received Mar 11, 2019; accepted Apr 6, 2019.

Supplementary material cited in this article is available online at https://doi.org/10.1016/j.bpsc.2019.04.004.

REFERENCES

1. Insel TR (2010): Rethinking schizophrenia. Nature 468:187–193.
2. Gore FM, Bloem PJ, Patton GC, Ferguson J, Joseph V, Coffey C, *et al.* (2011): Global burden of disease in young people aged 10-24 years: A systematic analysis. Lancet 377:2093–2102.
3. Fusar-Poli P, Borgwardt S, Bechdolf A, Addington J, Riecher-Rössler A, Schultze-Lutter F, *et al.* (2013): The psychosis high-risk state. JAMA Psychiatry 70:107–120.
4. Kremen WS, Vinogradov S, Poole JH, Schaefer CA, Deicken RF, Factor-Litvak P, Brown AS (2010): Cognitive decline in schizophrenia from childhood to midlife: A 33-year longitudinal birth cohort study. Schizophr Res 118:1–5.
5. Marín O (2016): Developmental timing and critical windows for the treatment of psychiatric disorders. Nat Med 22:1229–1238.
6. Rapoport JL, Giedd JN, Gogtay N (2012): Neurodevelopmental model of schizophrenia: Update 2012. Mol Psychiatry 17:1228–1238.
7. Yung AR, Yuen HP, McGorry PD, Phillips LJ, Kelly D, Dell'Olio M, *et al.* (2005): Mapping the onset of psychosis: The Comprehensive Assessment of At-Risk Mental States. Aust N Z J Psychiatry 39:964–971.
8. Millan MJ, Andrieux A, Bartzokis G, Cadenhead K, Dazzan P, Fusar-Poli P, *et al.* (2016): Altering the course of schizophrenia: Progress and perspectives. Nat Rev Drug Discov 15:485–515.
9. Yung AR, Stanford C, Cosgrave E, Killackey E, Phillips L, Nelson B, McGorry PD (2006): Testing the Ultra High Risk (prodromal) criteria for the prediction of psychosis in a clinical sample of young people. Schizophr Res 84:57–66.
10. Fusar-Poli P, Bonoldi I, Yung AR, Borgwardt S, Kempton MJ, Valmaggia L, *et al.* (2012): Predicting psychosis: Meta-analysis of transition outcomes in individuals at high clinical risk. Arch Gen Psychiatry 69:220–229.
11. Nelson B, Amminger GP, Yuen HP, Wallis N, J Kerr M, Dixon L, *et al.* (2018): Staged Treatment in early psychosis: A sequential multiple assignment randomised trial of interventions for ultra high risk of psychosis patients. Early Interv Psychiatry 12:292–306.
12. Schmidt SJ, Schultze-Lutter F, Schimmelmann BG, Maric NP, Salokangas RK, Riecher-Rössler A, *et al.* (2015): EPA guidance on the early intervention in clinical high risk states of psychoses. Eur Psychiatry 30:388–404.
13. Kapur S, Phillips AG, Insel TR (2012): Why has it taken so long for biological psychiatry to develop clinical tests and what to do about it. Mol Psychiatry 17:1174–1179.
14. Schneider M, Debbané M, Bassett AS, Chow EWC, Fung WLA, van den Bree MBM, *et al.* (2014): Psychiatric disorders from childhood to adulthood in 22q11.2 deletion syndrome: Results from the International Consortium on Brain and Behavior in 22q11.2 Deletion Syndrome. Am J Psychiatry 171:627–639.
15. Bassett AS, Chow EWC (1999): 22q11 deletion syndrome: A genetic subtype of schizophrenia. Biol Psychiatry 46:882–891.
16. Schneider M, Armando M, Pontillo M, Vicari S, Debbané M, Schultze-Lutter F, Eliez S (2016): Ultra high risk status and transition to psychosis in 22q11.2 deletion syndrome. World Psychiatry 15:259–265.
17. Gothelf D, Feinstein C, Thompson T, Gu E, Penniman L, Van Stone E, *et al.* (2007): Risk factors for the emergence of psychotic disorders in adolescents with 22q11.2 deletion syndrome. Am J Psychiatry 164:663–669.
18. Gothelf D, Schneider M, Green T, Debbané M, Frisch A, Glaser B, *et al.* (2013): Risk factors and the evolution of psychosis in 22q11.2 deletion syndrome: A longitudinal 2-site study. J Am Acad Child Adolesc Psychiatry 52:1192–1203.e3.
19. Satterthwaite TD, Baker JT (2015): How can studies of resting-state functional connectivity help us understand psychosis as a disorder of brain development? Curr Opin Neurobiol 30:85–91.
20. Van Den Heuvel MP, Fornito A (2014): Brain networks in schizophrenia. Neuropsychol Rev 24:32–48.
21. Chang C, Glover GH (2010): Time-frequency dynamics of resting-state brain connectivity measured with fMRI. Neuroimage 50:81–98.
22. Christoff K, Irving ZC, Fox KCR, Spreng RN, Andrews-Hanna JR (2016): Mind-wandering as spontaneous thought: A dynamic framework. Nat Rev Neurosci 17:718–731.
23. Preti MG, Bolton TAW, Van De Ville D (2017): The dynamic functional connectome: State-of-the-art and perspectives. Neuroimage 160:41–51.
24. Hutchison RM, Womelsdorf T, Gati JS, Everling S, Menon RS (2013): Resting-state networks show dynamic functional connectivity in awake humans and anesthetized macaques. Hum Brain Mapp 34:2154–2177.
25. Karahanoglu FI, Van De Ville D (2017): Dynamics of large-scale fMRI networks: Deconstruct brain activity to build better models of brain function. Curr Opin Biomed Eng 3:28–36.
26. Calhoun VD, Miller R, Pearlson G, Adali T (2014): The Chronnectome: Time-varying connectivity networks as the next frontier in fMRI data discovery. Neuron 84:262–274.
27. Buckholtz JW, Meyer-Lindenberg A (2012): Psychopathology and the human connectome: Toward a transdiagnostic model of risk for mental illness. Neuron 74:990–1004.
28. Fornito A, Zalesky A, Pantelis C, Bullmore ET (2012): Schizophrenia, neuroimaging and connectomics. Neuroimage 62:2296–2314.
29. Van Den Heuvel MP, Sporns O, Collin G, Scheewe T, Mandl RC, Cahn W, *et al.* (2013): Abnormal rich club organization and functional brain dynamics in schizophrenia. JAMA Psychiatry 70:783–792.
30. Damaraju E, Allen EA, Belger A, Ford JM, McEwen S, Mathalon DH, *et al.* (2014): Dynamic functional connectivity analysis reveals transient states of dysconnectivity in schizophrenia. Neuroimage Clin 5:298–308.
31. Du Y, Pearlson GD, Yu Q, He H, Lin D, Sui J, *et al.* (2016): Interaction among subsystems within default mode network diminished in schizophrenia patients: A dynamic connectivity approach. Schizophr Res 170:55–65.
32. Miller RL, Yaesoubi M, Turner JA, Mathalon D, Preda A, Pearlson G, *et al.* (2016): Higher dimensional meta-state analysis reveals reduced resting fMRI connectivity dynamism in schizophrenia patients. PLoS One 11:e0149849.
33. Su J, Shen H, Zeng LL, Qin J, Liu Z, Hu D (2016): Heredity characteristics of schizophrenia shown by dynamic functional connectivity analysis of resting-state functional MRI scans of unaffected siblings. Neuroreport 27:843–848.
34. Sakoglu Ü, Pearlson GD, Kiehl KA, Wang YM, Michael AM, Calhoun VD (2010): A method for evaluating dynamic functional network connectivity and task-modulation: Application to schizophrenia. MAGMA 23:351–366.

35. Pelletier-Baldelli A, Andrews-Hanna JR, Mittal VA (2018): Resting state connectivity dynamics in individuals at risk for psychosis. J Abnorm Psychol 127:314–325.
36. Du Y, Fryer SL, Fu Z, Lin D, Sui J, Chen J, *et al.* (2018): Dynamic functional connectivity impairments in early schizophrenia and clinical high-risk for psychosis. Neuroimage 180:632–645.
37. Debbané M, Lazouret M, Lagioia A, Schneider M, Van De Ville D, Eliez S (2012): Resting-state networks in adolescents with 22q11.2 deletion syndrome: Associations with prodromal symptoms and executive functions. Schizophr Res 139:33–39.
38. Scariati E, Schaer M, Richiardi J, Schneider M, Debbané M, Van De Ville D, Eliez S (2014): Identifying 22q11.2 deletion syndrome and psychosis using resting-state connectivity patterns. Brain Topogr 27:808–821.
39. Mattiaccio LM, Coman IL, Schreiner MJ, Antshel KM, Fremont WP, Bearden CE, Kates WR (2016): Atypical functional connectivity in resting-state networks of individuals with 22q11.2 deletion syndrome: Associations with neurocognitive and psychiatric functioning. J Neurodev Disord 8:2.
40. Schreiner M, Forsyth JK, Karlsgodt KH, Anderson AE, Hirsh N, Kushan L, *et al.* (2017): Intrinsic connectivity network-based classification and detection of psychotic symptoms in youth with 22q11.2 deletions. Cereb Cortex 27:3294–3306.
41. Mattiaccio LM, Coman IL, Thompson CA, Fremont WP, Antshel KM, Kates WR (2018): Frontal dysconnectivity in 22q11.2 deletion syndrome: An atlas-based functional connectivity analysis. Behav Brain Funct 14:2.
42. Padula MC, Schaer M, Scariati E, Schneider M, Van De Ville D, Debbané M, Eliez S (2015): Structural and functional connectivity in the default mode network in 22q11.2 deletion syndrome. J Neurodev Disord 7:23.
43. Schreiner MJ, Karlsgodt KH, Uddin LQ, Chow C, Congdon E, Jalbrzikowski M, Bearden CE (2014): Default mode network connectivity and reciprocal social behavior in 22q11.2 deletion syndrome. Soc Cogn Affect Neurosci 9:1261–1267.
44. Zöller D, Schaer M, Scariati E, Padula MC, Eliez S, Van De Ville D (2017): Disentangling resting-state BOLD variability and PCC functional connectivity in 22q11.2 deletion syndrome. Neuroimage 149:85–97.
45. Zöller D, Padula MC, Sandini C, Schneider M, Scariati E, Van De Ville D, *et al.* (2017): Psychotic symptoms influence the development of anterior cingulate BOLD variability in 22q11.2 deletion syndrome. Schizophr Res 193:319–328.
46. Padula MC, Scariati E, Schaer M, Eliez S (2018): A mini review on the contribution of the anterior cingulate cortex in the risk of psychosis in 22q11.2 deletion syndrome. Front Psychiatry 9:9–14.
47. Kapur S (2003): Psychosis as a state of aberrant salience: A framework linking biology, phenomenology, and pharmacology in schizophrenia. Am J Psychiatry 160:13–23.
48. Leonardi N, Van De Ville D (2015): On spurious and real fluctuations of dynamic functional connectivity during rest. Neuroimage 104:430–436.
49. Liu C, Xue Z, Palaniyappan L, Zhou L, Liu H, Qi C, *et al.* (2016): Abnormally increased and incoherent resting-state activity is shared between patients with schizophrenia and their unaffected siblings. Schizophr Res 171:158–165.
50. Karahanoglu FI, Van De Ville D (2015): Transient brain activity disentangles fMRI resting-state dynamics in terms of spatially and temporally overlapping networks. Nat Commun 6:7751.
51. Zöller DM, Bolton TA, Karahanoglu FI, Eliez S, Schaer M, Van De Ville D (2019): Robust recovery of temporal overlap between network activity using transient-informed spatio-temporal regression. IEEE Trans Med Imaging 38:291–302.
52. Miller TJ, Mcglashan TH, Rosen JL, Cadenhead K, Ventura J, Mcfarlane W, *et al.* (2003): Prodromal assessment with the Structured Interview for Prodromal Syndromes and the Scale of Prodromal Symptoms: Predictive validity, interrater reliability, and training to reliability. Schizophr Bull 29:703–715.
53. Achenbach TM (1991): Manual for the Child Behavior Checklist/4-18 and 1991 Profile. Burlington, NJ: University of Vermont Department of Psychiatry.
54. Achenbach TM, Rescorla LA (2003): Manual for the ASEBA Adult Forms & Profiles. Burlington, VT: University of Vermont, Research Center for Children, Youth, & Families.
55. Yan Chaogan ZY (2010): DPARSF: A MATLAB toolbox for "pipeline" data analysis of resting-state fMRI. Front Syst Neurosci 4:13.
56. Aleman-Gomez Y, Melie-García L, Valdés-Hernandez P (2006): IBASPM: Toolbox for automatic parcellation of brain structures. In: Presented at the 12th Annual Meeting of the Organization for Human Brain Mapping, June 11–15, Florence, Italy.
57. Ashburner J, Friston KJ (2005): Unified segmentation. Neuroimage 26:839–851.
58. Ashburner J (2007): A fast diffeomorphic image registration algorithm. Neuroimage 38:95–113.
59. Power JD, Barnes KA, Snyder AZ, Schlaggar BL, Petersen SE (2012): Spurious but systematic correlations in functional connectivity MRI networks arise from subject motion. Neuroimage 59:2142–2154.
60. Karahanoglu FI, Bayram I, Van De Ville D (2011): A signal processing approach to generalized 1-D total variation. IEEE Trans Sig Process 59:5265–5274.
61. Karahanoglu FI (2013): Sparsity-promoting spatiotemporal regularization for data mining in functional magnetic resonance imaging. Available at: https://infoscience.epfl.ch/record/187927. Accessed November 14, 2018.
62. Farouj Y, Karahanoglu FI, Van De Ville D (2017): Regularized spatiotemporal deconvolution of fMRI data using gray-matter constrained total variation. In: Proceedings of the 14th IEEE International Symposium on Biomedical Imaging: From Nano to Macro (ISBI'17). Piscataway, NJ. IEEE, 472–475.
63. Karahanoglu FI, Caballero-Gaudes C, Lazeyras F, Van De Ville D (2013): Total activation: FMRI deconvolution through spatio-temporal regularization. Neuroimage 73:121–134.
64. Krishnan A, Williams LJ, McIntosh AR, Abdi H (2011): Partial least squares (PLS) methods for neuroimaging: A tutorial and review. Neuroimage 56:455–475.
65. Etkin A, Wager T (2007): Reviews and overviews functional neuroimaging of anxiety: A meta-analysis of emotional processing in PTSD, social anxiety disorder, and specific phobia. Am J Psychiatry 164:1476–1488.
66. Menon V (2011): Large-scale brain networks and psychopathology: A unifying triple network model. Trends Cogn Sci 15:483–506.
67. McDonald-McGinn DM, Sullivan KE, Marino B, Philip N, Swillen A, Vorstman JAS, *et al.* (2015): 22q11.2 deletion syndrome. Nat Rev Dis Primers 1:15071.
68. LeDoux JE (2000): Emotion circuits in the brain. Annu Rev Neurosci 23:155–184.
69. Pessoa L (2008): On the relationship between emotion and cognition. Nat Rev Neurosci 9:148–158.
70. Ottet M-C, Schaer M, Debbané M, Cammoun L, Thiran J-P, Eliez S (2013): Graph theory reveals dysconnected hubs in 22q11DS and altered nodal efficiency in patients with hallucinations. Front Hum Neurosci 7:402.
71. Sandini C, Scariati E, Padula MC, Schneider M, Schaer M, Van De Ville D, Eliez S (2017): Cortical dysconnectivity measured by structural covariance is associated with the presence of psychotic symptoms in 22q11.2 deletion syndrome. Biol Psychiatry Cogn Neurosci Neuroimaging 3:433–442.
72. Sandini C, Zöller D, Scariati E, Padula MC, Schneider M, Schaer M, *et al.* (2018): Development of structural covariance from childhood to adolescence: A longitudinal study in 22q11.2DS. Front Neurosci 12:327.
73. Scariati E, Schaer M, Karahanoglu FI, Schneider M, Richiardi J, Debbané M, *et al.* (2016): Large-scale functional network reorganization in 22q11.2 deletion syndrome revealed by modularity analysis. Cortex 82:86–99.
74. Váša F, Griffa A, Scariati E, Schaer M, Urben S, Eliez S, Hagmann P (2016): An affected core drives network integration deficits of the structural connectome in 22q11.2 deletion syndrome. Neuroimage Clin 10:239–249.

75. Wig GS (2017): Segregated systems of human brain networks. Trends Cogn Sci 21:981–996.
76. Kohno T, Shiga T, Kusumi I, Matsuyama T, Kageyama H, Katoh C, *et al.* (2006): Left temporal perfusion associated with suspiciousness score on the Brief Psychiatric Rating Scale in schizophrenia. Psychiatry Res Neuroimaging 147:163–171.
77. Malaspina D, Storer S, Furman V, Esser P, Printz D, Berman A, *et al.* (1999): SPECT study of visual fixation in schizophrenia and comparison subjects. Biol Psychiatry 46:89–93.
78. Li Z, Lei W, Deng W, Zheng Z, Li M, Ma X, *et al.* (2017): Aberrant spontaneous neural activity and correlation with evoked-brain potentials in first-episode, treatment-naïve patients with deficit and non-deficit schizophrenia. Psychiatry Res Neuroimaging 261:9–19.
79. Seeley WW, Menon V, Schatzberg AF, Keller J, Glover GH, Kenna H, *et al.* (2007): Dissociable intrinsic connectivity networks for salience processing and executive control. J Neurosci 27:2349–2356.
80. Britz J, Van De Ville D, Michel CM (2010): BOLD correlates of EEG topography reveal rapid resting-state network dynamics. Neuroimage 52:1162–1170.
81. Rieger K, Hernandez LD, Baenninger A, Koenig T (2016): 15 years of microstate research in schizophrenia - Where are we? A meta-analysis. Front Psychiatry 7:22.
82. Tomescu MI, Rihs TA, Becker R, Britz J, Custo A, Grouiller F, *et al.* (2014): Deviant dynamics of EEG resting state pattern in 22q11.2 deletion syndrome adolescents: A vulnerability marker of schizophrenia? Schizophr Res 157:175–181.
83. Tomescu MI, Rihs TA, Roinishvili M, Karahanoglu FI, Schneider M, Menghetti S, *et al.* (2015): Schizophrenia patients and 22q11.2 deletion syndrome adolescents at risk express the same deviant patterns of resting state EEG microstates: A candidate endophenotype of schizophrenia. Schizophr Res Cogn 2:159–165.
84. Dufour F, Schaer M, Debbané M, Farhoumand R, Glaser B, Eliez S (2008): Cingulate gyral reductions are related to low executive functioning and psychotic symptoms in 22q11.2 deletion syndrome. Neuropsychologia 46:2986–2992.
85. Tovote P, Fadok JP, Lüthi A (2015): Neuronal circuits for fear and anxiety. Nat Rev Neurosci 16:317–331.
86. Davis M, Walker DL, Miles L, Grillon C (2010): Phasic vs sustained fear in rats and humans: Role of the extended amygdala in fear vs anxiety. Neuropsychopharmacology 35:105–135.
87. Maren S, Quirk GJ (2004): Neuronal signalling of fear memory. Nat Rev Neurosci 5:844–852.
88. Fox AS, Kalin NH (2014): A translational neuroscience approach to understanding the development of social anxiety disorder and its pathophysiology. Am J Psychiatry 171:1162–1173.
89. Fox AS, Oler JA, Shelton SE, Nanda SA, Davidson RJ, Roseboom PH, Kalin NH (2012): Central amygdala nucleus (Ce) gene expression linked to increased trait-like Ce metabolism and anxious temperament in young primates. Proc Natl Acad Sci U S A 109:18108–18113.
90. Fox AS, Shelton SE, Oakes TR, Davidson RJ, Kalin NH (2008): Trait-like brain activity during adolescence predicts anxious temperament in primates. PLoS One 3:e2570.
91. Kaczkurkin AN, Moore TM, Ruparel K, Ciric R, Calkins ME, Shinohara RT, *et al.* (2016): Elevated amygdala perfusion mediates developmental sex differences in trait anxiety. Biol Psychiatry 80:775–785.
92. Etkin A, Büchel C, Gross JJ (2015): The neural bases of emotion regulation. Nat Rev Neurosci 16:693–700.
93. Milad MR, Quirk GJ (2002): Neurons in medial prefrontal cortex signal memory for fear extinction. Nature 420:70–74.
94. Quirk GJ, Likhtik E, Pelletier JG, Paré D (2003): Stimulation of medial prefrontal cortex decreases the responsiveness of central amygdala output neurons. J Neurosci 23:8800–8807.
95. Vidal-Gonzalez I, Vidal-Gonzalez B, Rauch SL, Quirk GJ (2006): Microstimulation reveals opposing influences of prelimbic and infralimbic cortex on the expression of conditioned fear. Learn Mem 13:728–733.
96. Corcoran KA, Quirk GJ (2007): Activity in prelimbic cortex is necessary for the expression of learned, but not innate, fears. J Neurosci 27:840–844.
97. Courtin J, Chaudun F, Rozeske RR, Karalis N, Gonzalez-Campo C, Wurtz H, *et al.* (2014): Prefrontal parvalbumin interneurons shape neuronal activity to drive fear expression. Nature 505:92–96.
98. Burgos-Robles A, Vidal-Gonzalez I, Quirk GJ (2009): Sustained conditioned responses in prelimbic prefrontal neurons are correlated with fear expression and extinction failure. J Neurosci 29:8474–8482.
99. Power JD, Mitra A, Laumann TO, Snyder AZ, Schlaggar BL, Petersen SE (2014): Methods to detect, characterize, and remove motion artifact in resting state fMRI. Neuroimage 84:320–341.
100. Wechsler D (1991): Weschler Intelligence Scale for Children. San Antonio, TX: Psychological Corporation.
101. Wechsler D (1997): Wechsler Intelligence Scale for Adults. London, UK: Psychological Corporation.